

Composites of Cationic Nanofibrillated Cellulose and Layered Silicates: Water Vapor Barrier and Mechanical Properties

Thao T. T. Ho,^{*,†} Tanja Zimmermann,[†] Steffen Ohr,[‡] and Walter R. Caseri[§]

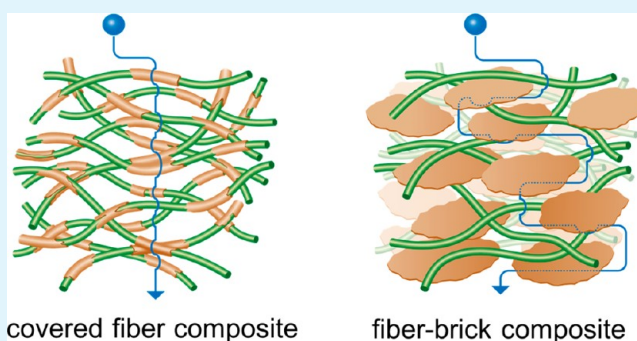
[†]Applied Wood Materials, Empa, Swiss Federal Laboratories for Materials Science and Technology, 8600 Duebendorf, Switzerland

[‡]Cham-Tenero Paper Mills Inc., 6330 Cham, Switzerland

[§]Department of Materials, Eidgenössische Technische Hochschule (ETH Zürich), 8093 Zürich, Switzerland

ABSTRACT: Composites of trimethylammonium-modified nanofibrillated cellulose and layered silicates (TMA-NFC/LS) were prepared by high-shear homogenization followed by pressure filtration and vacuum hot-pressing, which gave rise to particularly homogeneous dispersion of the silicate particles. Thirteen different clays and micas were employed. Water vapor barrier and mechanical properties (tensile strength, E-modulus, strain at break) of the composite films were investigated, considering the effects of layered silicate types and their concentration (in the range of 0 to 85 wt %). Good interactions between TMA-NFC and LS were obtained due to electrostatic attraction between cationic fibrils and anionic silicate layers, and even favored by high-shear homogenization process. Furthermore, oriented TMA-NFC/LS composite structure was achieved. Layered silicates exerted a pronounced influence on the water vapor barrier and mechanical properties; however, there was no common trend reflecting their types. The transport of water molecules through TMA-NFC/LS composites was studied considering both diffusion and adsorption mechanisms. As a result, diffusion pathways were proposed based on two new and one well-known models: the “native network”, “covered fiber composite”, and “fiber–brick composite” models. Importantly, it was found that the insertion of layered silicate particles did not improve automatically the barrier properties as indicated by the commonly used “fiber–brick composite” model. Mica R120 at a 50 wt % loading in composites with TMA-NFC matrix showed 30-fold improved water vapor permeability and 5-fold higher E-modulus compared to commercially used base paper.

KEYWORDS: cationic nanofibrillated cellulose (TMA-NFC), layered silicate (LS), water vapor transmission rate (WVTR), water vapor permeability (WVP), water vapor adsorption (WVA), diffusion, adsorption



1. INTRODUCTION

Paper and board based on cellulose take up around 40% of the global packaging market. Unfortunately, cellulose restricts the barrier properties in packaging applications because cellulose paper is highly permeable to water vapor and oxygen. During the last decades, however, nanofibrillated cellulose (NFC) has become available. NFC is produced from cellulose fibers by chemical, enzymatic, or mechanical treatment or combinations thereof.^{1–3} Compared to cellulose fibers, NFC has a particularly high grade of homogeneity, high tensile strength and modulus, high aspect ratio, and high chemical reactivity due to the presence of –OH groups at large specific surface area.^{4–6} Recently, it has been reported that the oxygen barrier properties of nanofibrillated cellulose films are superior to those of films composed of cellulose fibers, reaching oxygen transmission rates of 18 cm³/(m²·d) or oxygen permeability of 0.05 (cm³ mm)/(m² day atm) at 50% relative humidity (RH) and a temperature of 23 °C.^{7,8} It is likely that the diffusion of oxygen molecules through the NFC network is restricted by the dense network of interfibrillar bonds.^{6,8} However, water vapor barrier properties of such films were shown to be poor.⁹

To improve the water barrier properties, researchers have chemically modified cellulose, e.g., by acetylation^{9,10} or silylation.¹¹ In another approach, cellulose or its derivatives have been mixed with clay minerals.^{12–14} For instance, composites of cellulose acetate butyrate (CAB) and 3 wt % surface modified “organoclay” showed a decrease in water vapor transmission rate of about 20% compared to blank CAB films.¹⁵ In another example, the inclusion of organoclay in cellulose acetate showed a pronounced decrease of the oxygen but not of the water vapor transmission rate.¹⁶ Similarly, the inclusion of clays in synthetic polymers, like polyimides,¹⁷ polymethacrylates,^{18,19} polyethylene,²⁰ or polystyrene^{19,21} also led to an enhancement of barrier properties, mostly in oxygen transmission. However, the use of layered silicates in NFC was rarely mentioned.^{7,22,23} The investigations on such composites have been mostly limited to montmorillonite as a silicate component, although various kinds of layered silicates are

Received: June 27, 2012

Accepted: August 28, 2012

Published: August 28, 2012

readily available, such as vermiculite, kaolin, talc, or micas. Notably, these silicates as well as the renewable resource cellulose are natural, eco-friendly materials.

Importantly, homogeneous dispersion of layered silicate platelets in cellulose is very challenging. Namely, cellulose carries negative charges ($-O^-$ and $-COO^-$ groups) that will repel the negatively charged surfaces of the silicate layers. Modification of clays with organic molecules is commonly used in order to increase the dispersibility of the otherwise highly polar ionic surfaces of clays in apolar polymer matrices, such as polyethylene, polypropylene or polystyrene.²⁴ However, these modifications cannot address the target of dispersion of clays or micas in a polar NFC matrix. Therefore, a strategy of cellulose cationization²⁵ has been recently suggested (Figure 1) to favor

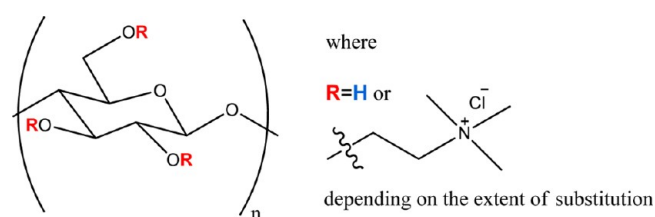


Figure 1. Structure of trimethylammonium-modified nanofibrillated cellulose (TMA-NFC).

electrostatic attractions between the cationic NFC (TMA-NFC) and negatively charged layered silicate platelets, which indeed led to high compatibility between these components.

In earlier studies, different morphologies as well as interaction behavior of layered silicates with TMA-NFC were observed.²⁶ This plays, however, a decisive role for the barrier properties of the ensuing composite films. Thus, for the discussion of the results obtained, three models have been distinguished. The neat NFC or TMA-NFC network will be assigned as “native network” model (Figure 2a). Remarkably, it was observed further that tissue-like montmorillonite flakes were bent and folded to cover the cationic cellulose fibrils.²⁶ The resulting composite system will be defined as “covered fiber composite” (Figure 2b). Finally, the flat layered silicates talc, kaolin, vermiculite, and mica platelets can build together with the NFC network a structure which is described with the well-known “fiber–brick composite” (Figure 2c). The “fiber–

brick composite” model is usually anticipated in the literature.^{27–29} Only recently, it has been shown that the “covered fiber composite” model can also exist.²⁶

Theoretically, the permeability (P) of low-molecular-weight species through a polymeric system can be described as the combination of the adsorption (A) and the diffusion coefficient (D) according to the following expression: $P = DA$.³⁰ The adsorption coefficient of a gaseous substance is related to the ratio of the equilibrium pressure of the adsorbing substance to its partial pressure in the gas phase. The diffusion coefficient, which can generally be determined from Fick’s laws of diffusion, characterizes the average ability of the permeant to move among the segments of composite materials.^{30,31} Different from the diffusion mechanism which depends on the composite structure (Figure 2), the adsorption is controlled by the interactions between penetrating molecules and the matrix. We would like to emphasize that the permeability of gases through composites of (nanofibrillated) cellulose and layered silicates has usually been treated solely on the basis of diffusion pathways,^{15,16,32} whereas adsorption was not considered.

In this study, various kinds of layered silicates were added as impermeable element to TMA-NFC matrices aiming at the production of composite films with improved water vapor barrier properties. Composite homogenization was achieved by application of shearing forces during high-pressure homogenization, which causes disintegration of layered silicate particles into thinner stacks or lamellae.²⁶ Pressure filtration and hot-pressing were used for producing TMA-NFC/layered silicate composite films. Barrier properties against water vapor as well as mechanical and morphological properties were investigated.

2. EXPERIMENTAL SECTION

2.1. Materials. Cellulose raw material was provided as Jelucel OF300 oat straw pulp powder from Jelu-Werke, Rosenberg, Germany. From this cellulose, trimethylammonium-modified nanofibrillated cellulose (TMA-NFC, Figure 1) was produced at 97.5 °C as described earlier.²⁵ The available cationic groups in TMA-NFC were calculated based on the nitrogen content (0.13 wt %), which is attributed to trimethylammonium groups. Thus, approximately, 0.015 cationic groups per anhydroglucose unit were present. Pretests showed that TMA-NFC underwent degradation at higher temperature (120 °C) resulting in reduced degree of polymerization. Therefore, in this study, only TMA-NFC modified at 97.5 °C has been used. Unmodified NFC

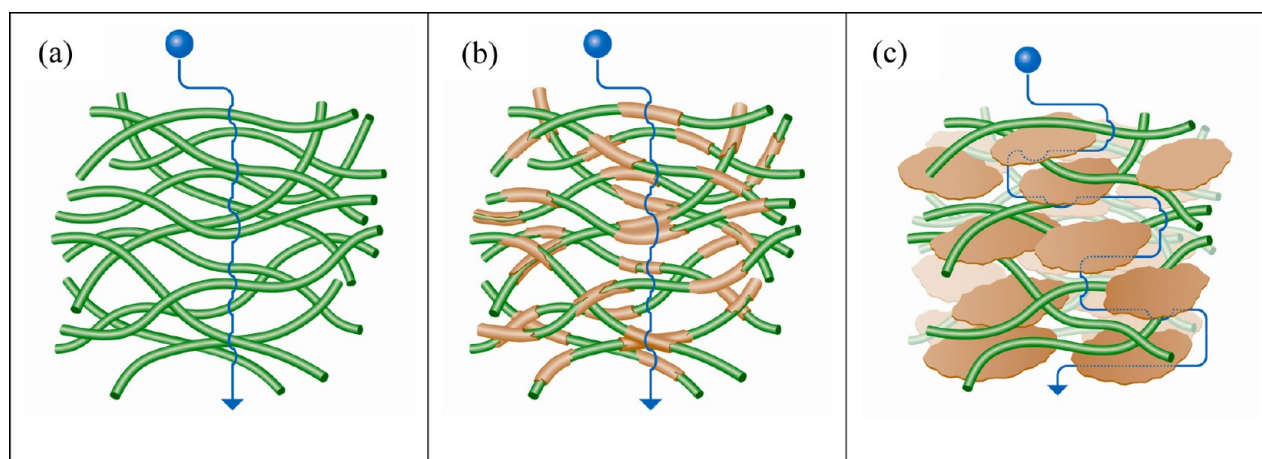


Figure 2. Schematic drawings of three model types: (a) neat NFC defined as “native network”, (b) “covered fiber composite” model, (c) the commonly used “fiber–brick composite” model. The diffusion pathway of a small molecule is illustrated with the blue line.

was also prepared for comparison. Besides elemental analysis, TMA-NFC was characterized in an earlier work²⁵ by methylene blue adsorption tests, X-ray powder diffraction, viscosity measurements and scanning electron microscopy.

Kraft-lux-2 was supplied by Cham-Tenero Paper Mills Inc. (Switzerland) as high quality reference paper, commonly used as base for packaging applications. It was prepared from a pulp mixture (50 wt %/50 wt %) of long fiber NBSK (long-fiber northern bleached softwood kraft pulp) and short fiber eucalyptus with addition of some starches and alkyl ketene dimer (AKD) sizing agent.

Thirteen different layered silicate types were used for the preparation of composites with TMA-NFC. The applied minerals represent all important groups of clay mineral families, i.e. smectite, talc, kaolin, vermiculite, and mica. Among those, different micas were considered as they showed potential highest improvements in water barrier properties in preliminary tests. These materials were characterized previously with respect to crystal structure, chemical composition, cation exchange capacity, density, specific surface area and morphology.²⁶ The list of clays and micas suppliers is presented in Table 1. Most of the investigated silicate layers are anionic.²⁶ However,

Table 1. Suppliers of Clays and Micas^a

name	supplier
Montmorillonite EXM1246	Süd-Chemie AG (Germany)
Kaolin Barrisurf HX	Imerys (France)
Talc	Erne-Chemie Dällikon (Switzerland)
Vermiculite grade 4	Virginia Vermiculite Limited (USA)
Mica PW30	Minelco (UK)
Mica R180	Microfine Minerals (UK)
Micavor 20	Kaolins d'Arvor (France)
Mica MU-M 2/1	Imerys (USA)
Mica SYA 31R	Alberto Luisoni AG (Switzerland)
Mica Sublime 325	Alberto Luisoni AG (Switzerland)
Rona Flair Silk Mica	Merck KGaA (Germany)
Mica SX400	Minelco (UK)
Mica R120	Minelco (UK)

^aNote that mica PW30 belongs to the phlogopite group, whereas the other mica samples are based on muscovite.

kaolin and talc surfaces are theoretically electrically neutral. Yet as they are natural products, they are contaminated by other silicates, leading to a cation exchange capacity (CEC) of ca. 2.5 (mEq/100 g of clay) for both minerals.

2.2. TMA-NFC/LS film preparation. Composites of TMA-NFC and layered silicates (LS) were prepared by high-shear homogenization, filtration and hot-press processes, as described previously.²⁶ For all films, a total mass of 4.41 g was always employed. For instance, in the case of a 1:1 mass ratio of cellulose and silicate, in the first step, 2.205 g of TMA-NFC and 2.205 g of clay or mica were put into separate flasks. Water was then added to the TMA-NFC until the total mass of the suspension reached 500 g. After that, this TMA-NFC suspension was transferred to a high pressure homogenizer (lab-scale microfluidizer type M-110Y, Microfluidics Corporation, USA)^{3,33} and subsequently pumped at high velocities through fixed-geometry interaction chambers (Y or Z morphology) with diameters of 200 μm (H30Z₂₀₀ μm) and 75 μm (F20Y₇₅ μm). Water was also added to the clay or mica, until the concentration in water reached 5 wt %. While TMA-NFC suspension was pumped in the homogenizer, the clay or mica suspension was added dropwise to the TMA-NFC suspension. The applied pressure was 1000 bar to generate the high shear forces necessary to disintegrate and homogenize the NFC and layered silicate materials. The final suspension was left to pass through the chambers for 20 times to homogenize the dispersion. Meanwhile, 200 mL of water had been added to the suspension, because NFC and clay or mica residues had to be collected from the flasks and the suspension container walls. The final concentration of TMA-NFC/LS in water was about 0.6 wt %.

The suspension was then transferred into a pressure filter, containing a twilled Dutch weave metal filter cloth (stainless steel AISI 316 L, 325 \times 2300 mesh) with pores size of 5 μm , supported by mechanically stable stainless steel mesh of larger pore size and a steel sheet with holes of 2.5 mm diameter. A pressure of 0.5 bar was applied in mounting steps until a stable but still wet film formed. The wet film together with the metal filter cloth was then encased in layers of blotting paper and one sheet of Teflon cloth was placed directly on the wet film, in order to prevent the blotting paper meshing with the sample. These layers were finally packed on a sheet of cotton and transferred into a vacuum bag.

A pump was connected to the vacuum bag and a vacuum (0.2 bar) was applied to remove water remnant, while the assembly was pressed at elevated temperatures by a Suter LP420 presser (A. Suter AG Maschinenbau, Basel, Switzerland) at 105 $^{\circ}\text{C}$ and 150 bar. After 25 min, the heat was turned off and the film was left to cool down while still under pressure to reduce residual stress. The cooling process lasted for about 2–3 h. The resulting composite films usually had a final concentration of layered silicates of 50 wt %. Nevertheless, in the case of mica R120 which was selected for investigation of the dependence of composite properties on layered silicate content, the TMA-NFC/mica R120 composite films had final contents of mica R120 from 0 to 85 wt %.

2.3. Characterization of TMA-NFC/LS Systems. **2.3.1. Water Vapor Barrier Tests.** The water vapor transmission rates (WVTR) of all films produced were measured by a VTI-SA+ dynamic vapor sorption analyzer (TA-Instruments, New Castle, USA). Silica gel was placed in a small cup with an inner diameter of 10 mm, an outer diameter of 15 mm, and a height of 10 mm, which was then sealed by a piece of NFC/LS film attached to the cup using double-sided adhesive tape. In general, the rate of water vapor transmission became linear in time after an initial period. Therefore, by measuring the mass gain of the silica gel over time under a controlled atmosphere, the WVTR could be calculated from the slope of a straight line obtained by linear regression of mass gain versus time and then by dividing the slope by the exposed area of the films. The temperature in the sample chamber was first adjusted to 60 $^{\circ}\text{C}$ at relative humidity (RH) of 0% within one hour and held there for another hour, in order to degas and equilibrate the sample. The chamber was then cooled to 23 $^{\circ}\text{C}$ within one hour. After a stable temperature (23 $^{\circ}\text{C}$) and envisaged relative humidity (85%) was reached, the mass measurement continued for another 90 min. In summary, the setup conditions in the chamber were 0% RH and 60 $^{\circ}\text{C}$ for drying; 85% RH and 23 $^{\circ}\text{C}$ for measuring. Some additional measurements for composite films with 50 wt % of mica R120 were performed at 50% RH and 23 $^{\circ}\text{C}$ for comparison.

The WVTR is typically given in units of $\text{mg}/(\text{min cm}^2)$, which can be converted to $\text{g}/(\text{m}^2 \text{ day})$. The average values of three samples are given in the following. The WVTR was normalized into water vapor permeability (WVP), which takes into account both water vapor pressure differences across the film and film thicknesses.

The water vapor permeability was calculated based on WVTR according to the following formula^{5,34,35}

$$\text{WVP} = \frac{\text{WVTR}d}{\Delta p} \quad (1)$$

where d (m) is the thickness of the composite film, measured with a Tesamaster micrometer (Switzerland) with 0.001 mm resolution. The data refer to average values taken at several points of the films.

Δp (Pa), the vapor pressure difference across the film, becomes

$$\Delta p = p_{\text{out}} - p_{\text{in}} = \frac{p_s(\text{RH}_{\text{out}} - \text{RH}_{\text{in}})}{100} \quad (2)$$

where p_{out} (Pa) is the actual water vapor pressure at the upper side of the film (i.e., outside the cup, in the chamber), p_{in} (Pa) is the actual water vapor pressure underneath of the film (inside the cup), and p_s (Pa) is the saturation water vapor pressure at 23 $^{\circ}\text{C}$ (i.e., 2800 Pa³⁶).

RH_{out} (%) and RH_{in} (%) are the relative humidities at the upper side and underneath of the film, respectively. The measurements were performed at RH_{out} of 85% and RH_{in} of 0% on the two sides of the

films, respectively, as silica gel desiccant creates virtually 0% relative humidity.³⁷

To investigate the tightness of the device used for determination of the water vapor permeation, aluminum foil was used whose water permeation rate is by far below the detection limits.³⁸ However, a low WVTR or WVP value resulted also for aluminum foil (4 g of water vapor/(m² day) or 1×10^{-7} g of water vapor/(m day Pa), respectively, at 85% RH and 23 °C), possibly due to a leakage as the design of the test cup requires application of double-sided tape to fix the films. Basically, these values should be subtracted from the related data of the cellulose-based films. However, because the leakage value was small compared to the values of the cellulose samples with or without layered silicates, the leakage value was neglected.

2.3.2. Water Vapor Adsorption. All test specimens were conditioned in a climate chamber held constant at 85% RH and 20 °C for one week, whereupon the sample mass was steady. The sample mass was recorded before being completely dried at 105 °C for 3 days. The mass of the dried samples was also determined. The water uptake or water adsorption (wt %) was then calculated based on the ratio of the mass difference between the conditioned and dried samples to the dried sample mass.

2.3.3. Tensile Tests. Tensile tests of all films were performed with an Instron 5864 testing machine (High Wycombe, UK) equipped with a 100 N load cell. The films were cut into samples of 12 mm in length and 2 mm in width. Therefore, each sample had an area of 138 mm². Prior to testing, the samples were conditioned at 43% RH and 23 °C. A cross-head speed of 2 mm/min and a prestrain of 0.1–0.2 N were applied. The average strength and moduli values of 4–5 samples were calculated.

2.3.4. Scanning Electron Microscopy. The procedure for the preparation of samples for scanning electron microscopy (SEM) was similar as reported previously.²⁵ SEM images of suspensions and composite films were evaluated. In the case of NFC/LS suspensions, the pictures were taken after the homogenization step. Such samples were prepared from a diluted 0.05 wt % suspension of which 2–3 drops were placed on a sample holder. Samples of NFC/LS composite films were prepared by fracturing the films in liquid nitrogen. The pieces thus obtained were then fixed on a sample holder with the fracture area facing upward. All samples were sputter-coated directly with a platinum layer of about 8 nm (BAL-TEC MED 020 Modular High Vacuum Coating Systems, BAL-TEC AG, Liechtenstein) in Ar as a carrier gas at 5×10^{-2} mbar. SEM images were finally recorded with a FEI Nova NanoSEM 230 instrument (FEI, Hillsboro, Oregon, USA) at an accelerating voltage of 5 kV and a working distance of 5 mm.

3. RESULTS

A combination of high-shear homogenization, pressure filtration and vacuum hot-pressing was applied to prepare trimethylammonium-modified nanofibrillated cellulose/layered silicate (TMA-NFC/LS) films (for details, see the Experimental Section). This procedure not only provided homogeneous dispersion of the layered silicates in the TMA-NFC matrix but also induced delamination of layered silicates agglomerations into thinner lamellae thus improving the homogeneity of the composite, as shown recently.²⁶ The applied 13 layered silicate minerals belong to various groups (e.g., smectite, kaolin, talc, vermiculite, and mica) that possess different characteristics,²⁶ whereas montmorillonite is the only representative known so far to create composites according to the “covered fiber composite” model. Because of their abundance in nature (especially when comparing to montmorillonite) and particularly high aspect ratio and layer charge as well as pronounced platy morphology,³⁹ various micas were employed in this study.

3.1. Water Vapor Transmission and Adsorption Properties. Water barrier properties of composites are presented as water vapor transmission rate (WVTR), water vapor permeability (WVP), and water vapor adsorption (WVA)

values. Lower values of WVP represent better protection from moisture, while comparison of WVTR values has to be taken with care, especially when comparing materials of neither the same basis mass nor the same thickness. Notably, the thickness of the films depends on many factors, e.g. preparation method, content of the solids (cellulose and layered silicate), or the densities of their components. Amazingly, WVTR values have been commonly used for cellulose systems in literature,^{9,15,16,23,40} whereas the WVP was only occasionally employed.³²

To determine the optimum silicate content in TMA-NFC for improved barrier properties, the commercially available mica R120 was employed as a representative for a mica of the muscovite group. Mica R120 was found earlier to have pronounced interactions with TMA-NFC fibrils²⁶ and also performed best in preliminary tests. The fraction of mica was varied between 0 and 85 wt %, corresponding approximately to mica volume fractions between 0 and 32 vol % (50 wt % corresponds to about 22 vol%), whereas the volume of the layered silicates used here in composite films can be calculated based on their densities as previously reported.²⁶ As visible from Figure 3, the WVTR and WVP values did not depend

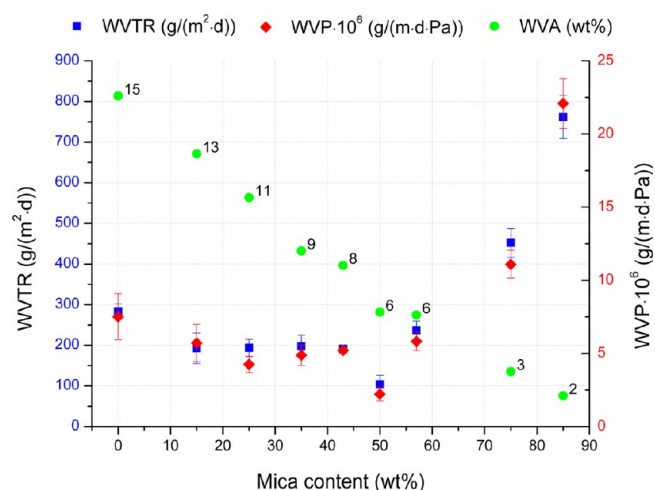


Figure 3. WVTR (left scale), WVP (right scale), and WVA (values above the dots) of composite films based on a TMA-NFC matrix plotted against the muscovite (mica R120) content. WVTR and WVP refer to 85% RH and 23 °C. Deviations are based on a 95% confidence level, using Student's t-distribution.

strikingly on the mica content up to about 60 wt %, but a reproducible minimum of WVTR value of 104 g of water vapor/(m² day) or WVP of 2.2×10^{-6} g of water vapor/(m day Pa) was found though at about 50 wt % mica. At higher mica fractions, the WVTR or WVP, respectively, rose sharply. Notice that all the values were measured at 85% RH and 23 °C (DIN 53122–1:2001). At 50% RH and 23 °C (TAPPI Test Method T4480m-09), however, TMA-NFC/mica R120 composites showed only a WVTR of 12 g of water vapor/(m²·d) and a WVP of 0.4×10^{-6} g of water vapor/(m·d·Pa). In opposite to water vapor transmission, WVA values were inversely proportional to the mica content, as seen in Figure 3.

Because WVP and WVTR reached a minimum at 50 wt % mica R120, films of TMA-NFC and other layered silicates were prepared with 50 wt % layered silicates. The related WVP and WVTR values results were presented in Table 2. First, it was obvious that the WVTR is a less reliable quantity than the WVP

Table 2. Water Vapor Permeability and Adsorption of Composite Films of TMA-NFC and 50 wt % Different Types of Layered Silicates (measured at 85% RH and 23 °C)^a

film sample	thickness (μm)	WVTR ($\text{g}/(\text{m}^2 \text{ day})$)	WVP $\cdot 10^6$ ($\text{g}/(\text{m day Pa})$)	WVA (wt %)
commercially used base paper	130 \pm 5	1087 \pm 170	59.4 \pm 9.6	12
nonmodified NFC	47 \pm 2	321 \pm 46	6.4 \pm 0.9	15
nonmodified NFC/Mica R120	52 \pm 1	260 \pm 66	5.7 \pm 1.5	7
TMA-NFC	63 \pm 12	284 \pm 18	7.5 \pm 1.6	15
TMA-NFC/Montmorillonite EXM1246	53 \pm 8	451 \pm 70	10.0 \pm 2.2	19
TMA-NFC/Kaolin Barrisurf HX	68 \pm 14	223 \pm 35	6.4 \pm 1.7	8
TMA-NFC/Talc	76 \pm 15	204 \pm 69	6.5 \pm 2.5	8
TMA-NFC/Vermiculite grade 4	67 \pm 3	189 \pm 17	5.3 \pm 0.5	12
TMA-NFC/Mica PW30	64 \pm 8	197 \pm 24	5.3 \pm 0.9	8
TMA-NFC/Mica R180	82 \pm 12	167 \pm 33	5.8 \pm 1.4	8
TMA-NFC/Micavor 20	119 \pm 20	262 \pm 51	13.1 \pm 3.4	8
TMA-NFC/Mica MU-M 2/1	55 \pm 5	359 \pm 16	83 \pm 0.8	8
TMA-NFC/Mica SYA 31R	46 \pm 5	221 \pm 89	4.3 \pm 1.8	7
TMA-NFC/Mica Sublime 325	51 \pm 7	184 \pm 19	3.9 \pm 0.7	7
TMA-NFC/Rona Flair Silk Mica	50 \pm 2	232 \pm 9	4.9 \pm 0.3	6
TMA-NFC/Mica SX400	78 \pm 2	323 \pm 17	10.6 \pm 0.6	8
TMA-NFC/Mica R120	51 \pm 1	104 \pm 22	2.2 \pm 0.5	6

^aFor comparison, the results for a commercially used base paper and neat non-modified and modified NFC films (i.e. without silicate) are also included. Deviations are based on a 95% confidence level, using Student's t-distribution.

because the former depends on the film thickness in contrast to the latter. Thus, for instance, the comparably high water vapor permeability of the materials with Micavor 20 is evident from the WVP but not from the WVTR values. As a consequence, we only refer to WVP values in the following.

Notably, the water vapor permeation of NFC films themselves was about an order of magnitude below that of the common commercially used base paper for packaging, i.e., NFC films are much more effective barrier materials toward water vapor than base paper. There was no significant difference between the water barrier properties of nonmodified NFC and TMA-NFC (see Table 2). However, it is evident that the WVP depended on the type of incorporated layered silicate, the differences amounting to a factor of 6. Remarkably, the incorporation of layered silicates can lead to an increase or decrease in WVP. The lowest water vapor permeation was obtained with mica R120, which improved almost 30 and 3 times compared to commercially used base paper and blank NFC films without layered silicate, respectively. Likewise, at 50 wt % silicate content, Sublime 325 and Rona Flair Silk micas showed a significant reduction of WVP. In contrast, some micas (muscovites SX400, MU-M 2/1, micavor 20, or mica R180) and clays (montmorillonite, kaolin, and talc) had no water vapor barrier improvement effect with respect to neat (modified) NFC. Some of these (e.g., montmorillonite, micavor

20, or mica SX400) induced even an increase in water vapor permeation. Interestingly, theories based on the “fiber–brick composite” model are generally used to explain improved barrier properties of polymer/clay composites.^{27–29} This theory focuses on a tortuous pathway of a permeant that must travel around the clay platelets in order to diffuse through the film. However, results that disagree with this model are evident from Table 2. Hence, inclusion of clay minerals does not always result in the improvement of barrier properties. Other models, like the proposed “covered fiber composite” model, or other factors (aspect ratio of the particles, layer shape and size, volume of layered silicates, etc.) must be considered. Therefore, we would like to emphasize that the frequently anticipated improvement of barrier properties by layered silicates according to the “fiber–brick composite” model is not guaranteed.

Nonmodified NFC and TMA-NFC had approximately the same water uptake level (15 wt %), somewhat more than commercially used base paper (12 wt %). The incorporation of 50 wt % of layered silicates led in most cases to a reduction in water uptake to about half the value of TMA-NFC (typical water adsorption of the composites 6–8 wt %). Again, the micas Sublime 325, Rona Flair Silk, R120, and also SYA 31R showed lower level of water adsorption compared to other layered silicates in composites with TMA-NFC. However, the composites containing vermiculite or montmorillonite adsorbed more water than those with the other silicates, the NFC-TMA/montmorillonite materials even more than neat NFC.

3.2. Mechanical Properties. The influence of the silicate content on mechanical properties was investigated for composite films with muscovite mica R120 as it performed best in water vapor barrier properties (see section 3.1). Tensile properties of the above composites with different fractions of muscovite mica R120 ranging from 0 to 85 wt % were investigated as summarized in Figure 4.

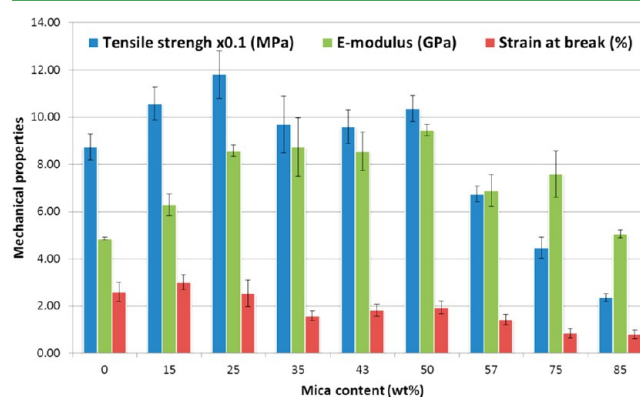


Figure 4. Tensile properties of TMA-NFC films comprising 0 to 85 wt % muscovite mica (R120). Deviations are based on a 95% confidence level, using Student's t-distribution.

The addition of mica up to a concentration of 25 wt % led to an increase in tensile strength and E-modulus without influencing the strain at break of the films. Only at higher mica concentrations well above 50 wt % the values of the tensile properties decreased, in particular the tensile strength and strain at break. The strain at break of composites declined with increase in mica content.

The composites of TMA-NFC and other layered silicates were also subject to investigations of tensile properties, as

summarized in Table 3. The commercially used base paper showed the lowest tensile strength (30 MPa) and E-modulus

Table 3. Tensile Properties (tensile strength, E-modulus, and strain at break) of Composite Films of TMA-NFC and 50 wt % Different Types of Layered Silicates^a

film sample	tensile strength (MPa)	E-modulus (GPa)	strain at break (%)
commercially used base paper	30 ± 2	1.8 ± 0.1	5.3 ± 0.6
nonmodified NFC	140 ± 6	6.4 ± 0.2	4.9 ± 0.6
nonmodified NFC/Mica R120	90 ± 3	7.3 ± 0.1	2.2 ± 0.2
TMA-NFC	87 ± 4	4.9 ± 0.1	2.6 ± 0.3
TMA-NFC/Montmorillonite EXM1246	116 ± 5	7.4 ± 0.6	3.0 ± 0.6
TMA-NFC/Kaolin Barrisurf HX	85 ± 12	6.6 ± 0.5	2.4 ± 0.7
TMA-NFC/Talc	67 ± 13	4.7 ± 0.2	2.9 ± 0.9
TMA-NFC/Vermiculite grade 4	90 ± 3	5.9 ± 0.5	4.1 ± 0.7
TMA-NFC/Mica PW30	56 ± 6	6.4 ± 1.0	1.1 ± 0.2
TMA-NFC/Mica R180	81 ± 20	6.6 ± 1.0	2.1 ± 0.6
TMA-NFC/Micavor 20	57 ± 3	3.8 ± 0.4	2.6 ± 0.2
TMA-NFC/Mica MU-M 2/1	62 ± 6	4.6 ± 0.3	2.2 ± 0.3
TMA-NFC/Mica SYA 31R	100 ± 8	9.8 ± 0.7	1.8 ± 0.2
TMA-NFC/Mica Sublime 325	68 ± 2	7.5 ± 0.3	1.4 ± 0.1
TMA-NFC/Rona Flair Silk Mica	111 ± 3	9.6 ± 0.3	2.3 ± 0.1
TMA-NFC/Mica SX400	50 ± 3	3.4 ± 0.1	2.7 ± 0.4
TMA-NFC/Mica R120	104 ± 5	9.5 ± 0.2	1.9 ± 0.3

^aFor comparison, commercially used base paper, non-modified NFC film, TMA-NFC film, and non-modified NFC/mica R120 film are also included. Deviations are based on a 95% confidence level, using Student's t-distribution.

(1.8 GPa) of all samples. Nonmodified NFC showed considerably higher values in tensile strength (140 MPa) and E-modulus (6.4 GPa), which were not reached by TMA-NFC. However, incorporation of layered silicates in TMA-NFC can result in lower or higher tensile strength and E-modulus compared to neat TMA-NFC. Thus, the highest tensile strength and E-modulus were found for TMA-NFC composite films with montmorillonite and three types of mica (SYA 31R, Rona Flair Silk, and R120) whereas the low values were obtained for other types of mica (for example, SX400 or MU-M 2/1). There was, therefore, no systematic dependence of tensile strength or E-modulus on the silicate type (mica vs clay).

For comparison, the mica leading to the composite with lowest WVP (mica R120) was also incorporated in non-modified NFC. Although this mica caused a reduction in tensile strength and only a slight improvement of E-modulus in nonmodified NFC, a significant increase in the related values was observed when TMA-NFC was used as matrix. Here, the E-modulus of TMA-NFC/mica R120 composite films performed even better than neat TMA-NFC films.

Although the strain at break values of the commercial base paper and nonmodified NFC did not differ significantly, the values decreased with utilization of TMA-NFC and the addition of layered silicates, with the exception of vermiculite. The strain at break values of the materials with layered silicates differed by a factor of 3.5 and, again, no systematic relationship was identified for the type of layered silicate (i.e., mica vs clay).

3.3. Morphology. To investigate the dispersibility of the particles of different layered silicate types in the aqueous suspensions used for composite preparation, SEM investigations were performed. Figure 5 shows dried suspensions of TMA-NFC/LS containing montmorillonite, vermiculite, and mica R120, respectively. It is evident that the montmorillonite particles (typical diameters 0.2–0.5 μm) were much finer than the vermiculite (typical diameters 0.3–4 μm) or mica R120 particles (typical diameters 0.5–9 μm). While montmorillonite with tissue-like shaped platelets folded around TMA-NFC fibrils, the other layered silicates with relatively flat and smooth platelets attached to TMA-NFC fibril surfaces.²⁶ The film fracture image (Figure 5d) shows that after filtration and hot-pressing, the mica platelets were oriented parallel to the surfaces of the composites.

4. DISCUSSION

The effects of layered silicate types and their concentrations on the composites' properties will be discussed in the following sections.

4.1. Layered Silicate Content in TMA-NFC. In general, low clay contents, typically less than 5 wt %, were used in clay/polymer composites.^{41,42} With TMA-NFC, however, composite films with high inorganic contents, i.e., 85 wt % or ca. 32 vol %, could be readily prepared. Such films were still self-supporting. It is most likely that the good interaction between cationic cellulose nanofibers and anionic layered silicate platelets²⁶ favor the existence of self-supporting films with high content of layered silicates. Good interaction between the cellulose nanofibrils and layered silicates was confirmed by SEM images, as discussed previously.²⁶ In addition, the composite systems which are prone to electrostatic attraction of opposite charges show better mechanical and water vapor properties, thus indicating that ionic interaction plays an important role.

4.1.1. Water Vapor Barrier Properties. Because of the excellent barrier properties of layered silicate itself, an increase in layered silicate content in composite systems is generally expected to cause a priori a decrease of water vapor transmission rate. We proved this theory for the system TMA-NFC/mica R120 and varied the mica content between 0 and 85 wt %. As expected, we observed a decrease in water vapor transmission, water vapor permeability, and water adsorption, however, only up to a certain extent, i.e., up to a mica concentration of around 50 wt % (ca. 22 vol %). Most probably, voids will appear in composites with very high mica content, as there is not sufficient matrix material to fill the spaces between the silicate particles. Furthermore, they widely differ in all three dimensions and therefore a void-free packing of the silicate particles themselves is not possible. In addition, we assume that very high amount of mica particles initiated formation of agglomerates, which caused defects in the material.

An increase in mica content, and respectively a decrease in TMA-NFC concentration in composites, led to a rather steady decrease of water adsorption per mass unit of composite as mica does not adsorb significant quantities of water vapor compared to cellulose. A decrease in TMA-NFC amount in the composites certainly leads to less available surface for water adsorption. Exceptionally, at 50 wt % mica, less than half of water uptake of neat TMA-NFC was found. The optimal water vapor barrier of TMA-NFC/mica R120 films at 50 wt % mica loading, confirmed the most sufficient interaction between

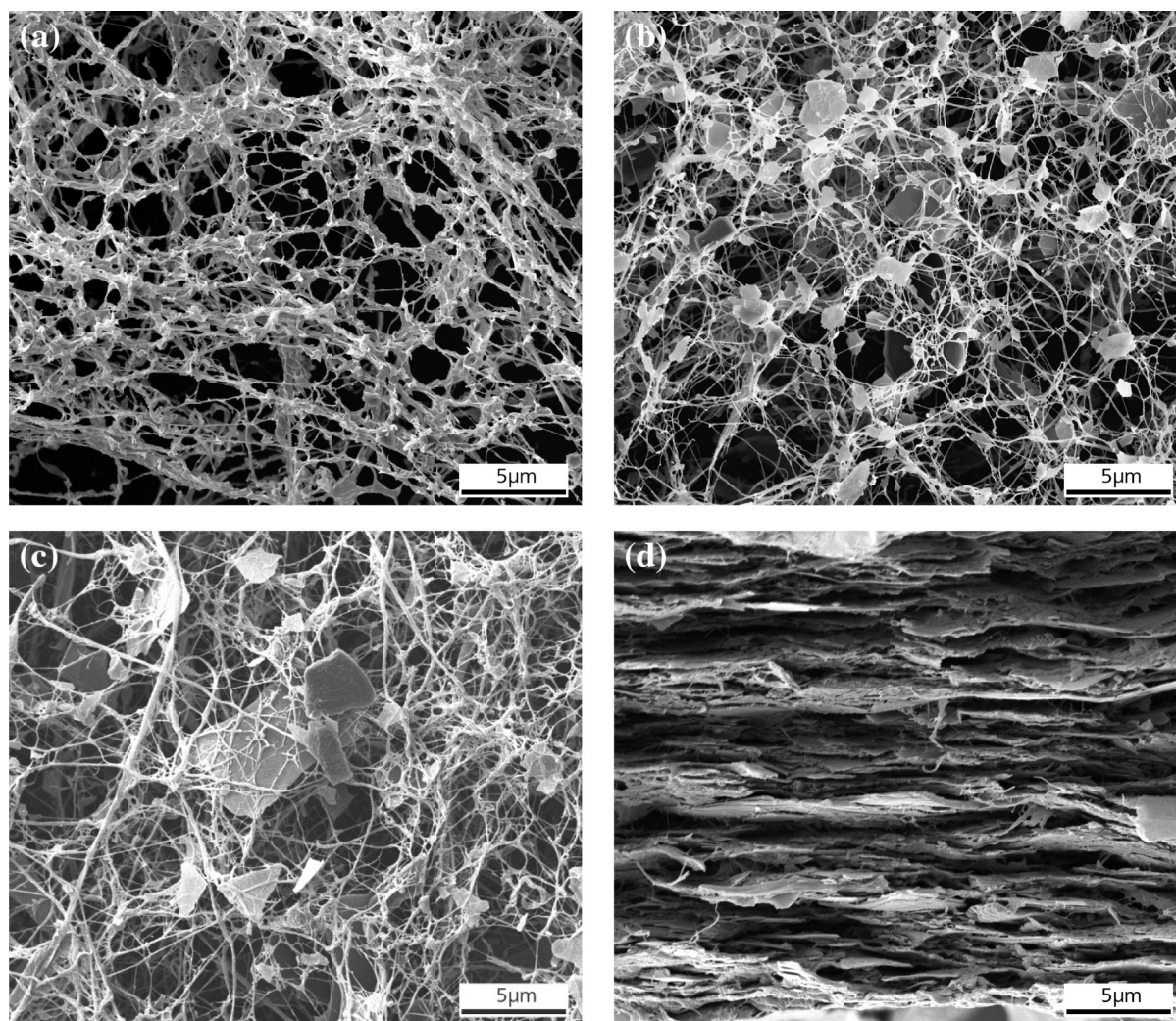


Figure 5. SEM images of (a) a dried suspension of TMA-NFC/montmorillonite, (b) a dried suspension of TMA-NFC/vermiculite, (c) a dried suspension of TMA-NFC/mica R120, and (d) a fracture surface of TMA-NFC/mica R120 film cross-section. All mentioned systems contain TMA-NFC and layered silicates in a mass ratio of 1:1.

TMA-NFC and mica platelets, which resulted in less cellulose surface available for water adsorption than in other cases.

4.1.2. Mechanical Properties. Different from many other polymer/clay composites, TMA-NFC/LS systems exhibited high E-moduli. An E-modulus of 27 MPa was reported for an epoxy resin with 15 wt % of an organically modified clay,⁴³ 1.57 GPa for polyethylene and 3 wt % of clay,⁴⁴ or 0.25 GPa for poly(lactic acid) (PLA) with 4 wt % of organically modified mica.⁴⁵ All these values are below the 6 GPa of TMA-NFC with 15 wt % of mica R120. Generally, it is not surprising that the addition of stiff clay particles to TMA-NFC results in an increase in E-modulus,¹³ probably because of good interactions between cationic cellulose fibrils and anionic mica platelets, which enable stress transfer to the mica platelets and therefore exploitation of their reinforcement effect.

It is likely that the reduction in E-modulus and tensile strength for more than ca. 50 wt % mica particles in TMA-NFC is caused by agglomerated particles disrupting the TMA-NFC network and acting as voids in the TMA-NFC/LS film. The strain at break of such highly loaded composites dropped with increase in mica content as the addition of highly rigid layered silicate material to NFC network restricts the movement of NFC chains. This also renders the composite films being more

brittle at higher mica fractions. In fact, a high amount of layered silicates is expected to disturb the interaction between cellulose fibrils and therefore reduces the tensile properties of the NFC film.

4.2. Type of Layered Silicate. Contrary to other studies which usually employed montmorillonite as filler for nano-fibrillated cellulose matrices,^{7,22,46} a broad spectrum of micas and clay minerals has been considered in our study.

4.2.1. Water Vapor Barrier Properties. As mentioned in the Introduction, permeability depends on both adsorption and diffusion (transmission) mechanisms. Adsorption of water is especially critical with regard to hydrophilic materials like cellulose. However, in most cases, only diffusion has usually been considered when referring the water vapor barrier of such materials.^{15,16,32} Even though the dense structure of NFC network hampers diffusion of water vapor, considerable quantities of water are adsorbed.

The diffusion pathway of a small molecule through a TMA-NFC/LS system (cf. Figure 2) depends on the layered silicate type and its interaction with TMA-NFC. Considering the diffusion pathway alone (without taking adsorption into account), nonmodified NFC, TMA-NFC, and even base paper can be attributed to the “native network” model, TMA-

NFC/montmorillonite to the “covered fiber composite” model, and TMA-NFC with the other layered silicates (kaolin, talc, vermiculite, mica) to the “fiber–brick composite” model.

According to the “native network” model, the permeation of water vapor through a native cellulose fiber network is an order of magnitude above that through the finer and denser NFC network. As the structure of the fiber material is retained in the “covered fiber composite” model, the water vapor permeation through TMA-NFC/montmorillonite is expected to be relatively high, and it was in fact even higher than in TMA-NFC. Besides a possible reduction in the packing density of montmorillonite-covered fibrils, high water adsorption might also contribute to the enhanced WVP. Notably, more water was adsorbed in the composites with montmorillonite than in TMA-NFC alone, as montmorillonite itself can take up water even in the silicate interlayers. This example alone shows already that incorporating layered silicates into NFC network cannot always ensure better barrier properties as frequently anticipated.

With regard to the WVP of the other layered silicates (i.e., kaolin, talc, vermiculite, and mica), no systematic dependence on the silicate chemical composition, cation exchange capacity, specific surface area, or density (the corresponding values were reported earlier)²⁶ was observed. Effects of silicate layer aspect ratios cannot be evaluated since, unfortunately, the aspect ratios of the layered silicate powders changed when embedded in NFC and cannot be measured reliably in the matrix. The diffusion pathway of small molecules becomes longer in presence of platelet mineral fillers (see Figure 2) but the often quoted argument that this automatically leads to a decrease in WVP has clearly been disproven by the above experiments.

Apart from the diffusion pathway, water adsorption has also to be considered. Cellulose pulp fibers used in base paper certainly provided at least an order of magnitude less surface –OH groups²⁵ compared to NFC or TMA-NFC. Because the difference in water uptake was much less than an order of magnitude, water obviously did not adsorb exclusively at the fiber surface but also within the fibers. The incorporation of 50 wt % layered silicates led in most cases to a reduction in water uptake to about half the value of TMA-NFC. This implies that those layered silicates did not adsorb considerable quantities of water, i.e., water adsorption was predominantly determined by the NFC matrix. As indicated above, montmorillonite can adsorb large quantities of water as the interlayer cations can be hydrated.^{47,48} On the basis of layer charge and chemical composition, vermiculite is related to montmorillonite as both minerals belong to 2:1 layer silicates with hydrated interlayer cations.⁴⁷ Therefore, vermiculite can also adsorb large amount of water, which is reflected in a high water uptake in composites with TMA-NFC. In contrast, the interlayer cations of micas are not hydrated, and accordingly their composites with TMA-NFC adsorb less water than those with montmorillonite or vermiculite.

Note that in this study, all water vapor barrier values were measured at 85% RH and 23 °C. WVTR values have been reported frequently at 50% RH.^{9,40} Certainly, these conditions would result in lower WVTR and WVP of composite films. This is illustrated by the fact that the WVP of TMA-NFC/mica R120 (at 50 wt %) at 50% RH and 23 °C, was 6 times less than the value at 85% RH and 23 °C. Therefore, TMA-NFC/mica R120 acts as an excellent water vapor barrier at moderate storage and usage conditions. Some WVTR and WVP data exist

for cellulose esters and synthetic polymers, but these have often been measured under different conditions and are thus difficult to compare. To provide a rough idea, cellulose acetate films exhibited WVTR of 2920 g/(m² day),³⁸ acetylated microfibrillated cellulose films of 167 g/(m² day) at 50% RH and 23 °C,⁹ and cellulose acetate/organo-montmorillonite of more than 900 g/(m² day) (measured at 37.8 °C and 100% RH).¹⁶ The TMA-NFC/layered silicate composites might be suitable for applications such as atmospheric packaging, short-term food packaging, or food packaging at specific storing conditions, e.g., at 15 °C and less than 70% RH.³⁴

4.2.2. Mechanical Properties. With regard to mechanical properties, the commercially used base paper showed the lowest tensile strength and E-modulus of all samples, because of the lower amount of possible fiber–fiber interactions compared to the interfibrillar bonding occurring between cellulose fibrils in NFC. Accordingly, TMA-NFC/layered silicate films showed significant mechanical property improvements.

Advantages of TMA-NFC matrices over nonmodified NFC were the cationic quaternary ammonium groups which ionically interacted with negative charges of layered silicates. The less favorable mechanical properties of composites with nonmodified NFC (i.e., without cationic groups) are most probably due to the absence of this specific interaction. The addition of layered silicate material into polymer matrix is expected to result in higher modulus and lower elongation at break of the final composites.¹³ This tendency is well-reflected in most TMA-NFC/LS systems with the exception of vermiculite and montmorillonite. This could be due to the high water adsorption ability of these layered silicates or in the case of montmorillonite to the specific morphology. Water entering the composite could act as a plasticizer,⁴⁹ possibly resulting in an increase in strain at break values.⁵⁰

Mechanical properties of TMA-NFC/LS were comparable to those of NFC films produced by Liu et al.⁴⁶ In contrast to our studies, NFC films from Liu et al. were not modified chemically and therefore the original degree of polymerization was preserved while the degree of polymerization of the TMA-NFC applied in this study was reduced by half compared to nonmodified NFC, as reported earlier.²⁵ Certainly, the degree of polymerization also depends strongly on the applied raw materials and disintegration processes. In addition, it has to be considered that the films prepared in this work and those by Liu et al. were tested under different conditions (e.g., temperature, humidity, testing machine speed, and film thickness).

It is evident that the composites of TMA-NFC and 50 wt % of mica R120 possess superior mechanical as well as water vapor barrier properties. This might originate in the pronounced interactions between anionic R120 platelets and cationic cellulose fibrils. Among the muscovites tested, R120 has the highest specific surface area and (exchangeable) potassium amount.²⁶ However, the above addressed properties are not always directly related to specific surface area and potassium amounts. Therefore, other factors such as layer aspect ratio or particle size distribution should also be taken into account, which are, however, difficult to quantify as already indicated above.

5. CONCLUSIONS

Various systems of cationic nanofibrillated cellulose and layered silicates were studied. Good interaction between cationic NFC and different layered silicate types was achieved. A multilayered

structure with homogeneously distributed silicate layers was obtained by using high-shear homogenization, pressure filtration as well as vacuum hot-press techniques. Most favorable water vapor permeability for barrier purposes among the material combinations tested was achieved with 50 wt % mica R120 in a TMA-NFC matrix. These materials also exhibited good mechanical properties (tensile strength and E-modulus). Remarkably, this TMA-NFC/mica R120 composite showed water vapor barrier improvement of almost 30 times compared to commercially used base paper and 3 times compared to blank TMA-NFC film at 85% RH. Notably, at 50% RH barrier against water vapor was even more effective.

Permeability of water vapor through the composite depends obviously on numerous factors. The frequently picture of the “fiber–brick composite” model to explain the water permeation through composites of polymer matrices and layered particles has shown to be too simple. Moreover, layered silicates do not form “fiber–brick composite” structures by necessity, as evident on the example of montmorillonite which establishes a “covered fiber composite” structure. Two new models are proposed and discussed in detail.

AUTHOR INFORMATION

Corresponding Author

*E-mail: thuthao.ho@empa.ch.

Notes

The authors declare no competing financial interest.

ACKNOWLEDGMENTS

We kindly acknowledge the Commission for Technology and Innovation (CTI) for financial support. We thank Esther Strub for performing SEM; Yee Song Ko for carrying out the mechanical tests. The help of Dr. Kirill Feldman, Dominik Meyer, and André Niederer is deeply appreciated. We are very grateful to Dr. Thomas Geiger, Dr. Philippe Tingaut, and Prof. Dominique Derome for their useful advices and support. Finally, we thank Prof. Paul Smith for valuable discussions.

REFERENCES

- (1) Iwamoto, S.; Nakagaito, A. N.; Yano, H. *Appl. Phys. A: Mater. Sci. Process* **2007**, *89*, 461–466.
- (2) Paakko, M.; Ankerfors, M.; Kosonen, H.; Nykanen, A.; Ahola, S.; Osterberg, M.; Ruokolainen, J.; Laine, J.; Larsson, P. T.; Ikkala, O.; Lindstrom, T. *Biomacromolecules* **2007**, *8*, 1934–1941.
- (3) Zimmermann, T.; Pöhler, E.; Geiger, T. *Adv. Eng. Mater.* **2004**, *6*, 754–761.
- (4) Eichhorn, S.; Dufresne, A.; Aranguren, M.; Marcovich, N.; Capadona, J.; Rowan, S.; Weder, C.; Thielemans, W.; Roman, M.; Renneckar, S.; Gindl, W.; Veigel, S.; Keckes, J.; Yano, H.; Abe, K.; Nogi, M.; Nakagaito, A.; Mangalam, A.; Simonsen, J.; Benight, A.; Bismarck, A.; Berglund, L.; Peijs, T. *J. Mater. Sci.* **2010**, *45*, 1–33.
- (5) Hubbe, M. A.; Rojas, O. J.; Lucia, L. A.; Sain, M. *BioResources* **2008**, *3*, 929–980.
- (6) Minelli, M.; Baschetti, M. G.; Doghieri, F.; Ankerfors, M.; Lindström, T.; Siró, I.; Plackett, D. *J. Membr. Sci.* **2010**, *358*, 67–75.
- (7) Liu, A.; Walther, A.; Ikkala, O.; Belova, L.; Berglund, L. A. *Biomacromolecules* **2011**, *12*, 633–641.
- (8) Syverud, K.; Stenius, P. *Cellulose* **2009**, *16*, 75–85.
- (9) Rodionova, G.; Lenes, M.; Eriksen, Ø.; Gregersen, Ø. *Cellulose* **2011**, *18*, 127–134.
- (10) Tingaut, P.; Zimmermann, T.; Lopez-Suevos, F. *Biomacromolecules* **2009**, *11*, 454–464.
- (11) Goussé, C.; Chanzy, H.; Cerrada, M. L.; Fleury, E. *Polymer* **2004**, *45*, 1569–1575.
- (12) White, Leslie A. *J. Appl. Polym. Sci.* **2004**, *92*, 2125–2131.

- (13) Ludvik, C.; Glenn, G.; Klamczynski, A.; Wood, D. *J. Polym. Environ.* **2007**, *15*, 251–257.
- (14) Sakran, M. *J. Radioanal. Nucl. Chem.* **1996**, *213*, 87–98.
- (15) Quintero, R. I.; Galotto, M. J.; Guarda, A.; Rodríguez, F., Mechanical, thermal, and water vapor barrier properties of nanocomposite films based on cellulose acetate butyrate. In *International Conference on Food Innovation – Food Innova 2010*; Universidad Politecnica de Valencia: Valencia, 2010.
- (16) Rodríguez, F. J.; Galotto, M. J.; Guarda, A.; Bruna, J. E. *J. Food Eng.* **2012**, *110*, 262–268.
- (17) Yano, K.; Usuki, A.; Okada, A. *J. Polym. Sci., Part A: Polym. Chem.* **1997**, *35*, 2289–2294.
- (18) Lee, D. C.; Jang, L. W. *J. Appl. Polym. Sci.* **1996**, *61*, 1117–1122.
- (19) Okamoto, M.; Morita, S.; Taguchi, H.; Kim, Y. H.; Kotaka, T.; Tateyama, H. *Polymer* **2000**, *41*, 3887–3890.
- (20) Lee, Y. H.; Park, C. B.; Sain, M.; Kontopoulou, M.; Zheng, W. *J. Appl. Polym. Sci.* **2007**, *105*, 1993–1999.
- (21) Fu, X.; Qutubuddin, S. *Mater. Lett.* **2000**, *42*, 12–15.
- (22) Sehaqui, H.; Liu, A. D.; Zhou, Q.; Berglund, L. A. *Biomacromolecules* **2010**, *11*, 2195–2198.
- (23) Spence, K. L.; Venditti, R. A.; Rojas, O. J.; Pawlak, J. J.; Hubbe, M. A. *BioResources* **2011**, *6*, 4370–4388.
- (24) Caseri, W. R. *Mater. Sci. Technol.* **2006**, *22*, 807–817.
- (25) Ho, T.; Zimmermann, T.; Hauert, R.; Caseri, W. *Cellulose* **2011**, *18*, 1391–1406.
- (26) Ho, T.; Ko, Y.; Zimmermann, T.; Geiger, T.; Caseri, W. *J. Mater. Sci.* **2012**, *47*, 4370–4382.
- (27) Nielsen, L. E. *J. Macromol. Sci., Chem.* **1967**, *1*, 929–942.
- (28) Rhim, J.-W.; Ng, P. K. W. *Crit. Rev. Food Sci. Nutr.* **2007**, *47*, 411–433.
- (29) Sinha Ray, S.; Okamoto, M. *Prog. Polym. Sci.* **2003**, *28*, 1539–1641.
- (30) Lagaron, J. M.; Catala, R.; Gavara, R. *Mater. Sci. Technol.* **2004**, *20*, 1–7.
- (31) Elias, H. G., *Macromolecules*; Wiley-VCH: Weinheim, Germany, 2005.
- (32) Park, H.-M.; Misra, M.; Drzal, L. T.; Mohanty, A. K. *Biomacromolecules* **2004**, *5*, 2281–2288.
- (33) Zimmermann, T.; Bordeanu, N.; Strub, E. *Carbohydr. Polym.* **2010**, *79*, 1086–1093.
- (34) Kaya, S.; Maskan, A. *J. Food Eng.* **2003**, *57*, 295–299.
- (35) Rhim, J. W. *Carbohydr. Polym.* **2011**, *86*, 691–699.
- (36) Ambrose, D.; Lawrenson, I. J. *J. Chem. Thermodyn. Thermochem.* **1972**, *4*, 755–761.
- (37) Chivrac, F.; Angellier-Coussy, H.; Guillard, V.; Pollet, E.; Avérous, L. *Carbohydr. Polym.* **2010**, *82*, 128–135.
- (38) Shogren, R. *J. Polym. Environ.* **1997**, *5*, 91–95.
- (39) Brindley, G. W.; Brown, G., *Crystal Structures of Clay Minerals and Their X-ray Identification*; Mineralogical Society: London, 1980.
- (40) Hult, E.-L.; Iotti, M.; Lenes, M. *Cellulose* **2010**, *17*, 575–586.
- (41) Adame, D.; Beall, G. W. *Appl. Clay Sci.* **2009**, *42*, 545–552.
- (42) Subramaniyan, A. K.; Sun, C. T. *Composites, Part A* **2006**, *37*, 2257–2268.
- (43) Shi, H.; Lan, T.; Pinnavaia, T. J. *Chem. Mater.* **1996**, *8*, 1584–1587.
- (44) Kato, M.; Okamoto, H.; Hasegawa, N.; Tsukigase, A.; Usuki, A. *Polym. Eng. Sci.* **2003**, *43*, 1312–1316.
- (45) Chen, B.; Evans, J. R. G.; Greenwell, H. C.; Boulet, P.; Coveney, P. V.; Bowden, A. A.; Whiting, A. *Chem. Soc. Rev.* **2008**, *37*, 568–594.
- (46) Liu, A.; Berglund, L. A. *Carbohydr. Polym.* **2012**, *87*, 53–60.
- (47) Bergaya, F.; Theng, B. K. G.; Lagaly, G. *Handbook of Clay Science*; Elsevier: Amsterdam, 2006; Vol. 1.
- (48) Murray, H. H. *Applied Clay Mineralogy: Occurrences, Processing, And Application of Kaolins, Bentonites, Palygorskite-Septiolite, and Common Clays*; Elsevier: Boston, 2007; p 180.
- (49) Kulachenko, A.; Denoyelle, T.; Galland, S.; Lindström, S. *Cellulose* **2012**, *19*, 793–807.
- (50) Bakar, M.; Djaidar, F. *J. Thermoplast. Compos. Mater.* **2007**, *20*, 53–64.